NOTICE
PORTIONS OF THIS REPORT ARE ILLEGIBLE.
It has been reproduced from the best available copy to permit the broadest possible availability.

CONF-840788--2

The ORNL ECR Multicharged Ion Source

CONF-840788--2

DE85 001283

F. W. Meyer

Oak Ridge National Laboratory,
Oak Ridge, TN 37831 USA

Proceedings of the
International Conference on the
Physics of Highly Ionised Atoms
Oxford, England
July 2-5, 1984

By acceptance of this article, the publisher or recipient acknowledges the U.S. Government's right to retain a nonexclusive, royalty-free license in and to any copyright covering the article.

DISCLAIMER

This report was prepared as an account of work sponsored by an agency of the United States Government. Neither the United States Government nor any agency thereof, nor any of their employees, makes any warranty, express or implied, or assumes any legal liability or responsibility for the accuracy, completeness, or usefulness of any information, apparatus, product, or process disclosed, or represents that its use would not infringe privately owned rights. Reference herein to any specific commercial product, process, or service by trade name, trademark, manufacturer, or otherwise does not necessarily constitute or imply its endorsement, recommendation, or favoring by the United States Government or any agency thereof. The views and opinions of authors expressed herein do not necessarily state or reflect those of the United States Government or any agency thereof.

MASTER

DISTRIBUTION OF THIS DOCUMENT IS UNLIMITED

The ORNL ECR Multicharged Ion Source*

F. W. Meyer

Oak Ridge National Laboratory, Oak Ridge, TN 37831 USA

Abstract

A multicharged ion source based on Electron Cyclotron Resonance (ECR) heating has been designed and built at ORNL. The ECR ion source, which is completely dedicated for atomic physics collision studies, produces higher charge states and higher beam intensities than the present ORNL PIG multicharged ion source, and will thus permit study of collision processes involving ions of higher charge states in experiments requiring higher beam intensities than could be previously obtained in our laboratory. The source has already produced up to fully stripped C and O beams, as well as up to He-like Ar beams. Measurements of the energy spread of ions extracted from the ion source operating in both single-stage and two-stage mode are described. In addition, initial results of total cross section measurements for fully stripped light ions incident on atomic hydrogen in the energy range 0.2-10 keV are presented.

I. Introduction

In order to be able to extend our ongoing studies of collisional interactions involving multicharged ions that are of interest to the magnetically-confined fusion program, a decision was made in 1981 to build an ECR multicharged ion source at ORNL. Multicharged ion sources based on Electron Cyclotron Resonance (ECR) heating have been demonstrated[1] to reliably produce significantly higher charge states than PIG type ion sources with the sufficiently high beam intensities and duty cycle required for the ion-electron and ion-atom crossed beams experiments in which we have recently been engaged.

---

*Research was supported by the Office of Fusion Energy of the U.S. Department of Energy under contract No. DE-AC05-84OR21400 with Martin Marietta Energy Systems, Inc.

Funding for the purchase of capital equipment related to the source was obtained in 1982 and 1983, during which time the bulk of the physics design was also carried out. The source engineering design and subsequent fabrication were carried out at ORNL during 1983. Construction and installation of the source were completed toward the end of 1983. Although the source was designed for operation at 10.6 GHz, initial source testing was carried out at 2.45 GHz in order to gain experience in source operation while awaiting delivery of the 10.6 GHz microwave amplifier scheduled for June 1984.

During the initial testing phase at 2.45 GHz, x-ray measurements of the bremsstrahlung spectrum produced by the source indicated the presence of electrons having energies up to 160 keV. Following construction and installation of the beam line and charge analyzer in March 1984, source performance could be assessed more directly by measuring charge state distributions of extracted beams. Even at the lower microwave frequency, fully stripped C beams were obtained, which were used to initiate the first planned experiment involving the new source, total cross sections measurements of electron capture by fully-stripped light ions incident on atomic hydrogen. Operation of the source at its design frequency of 10.6 GHz started on schedule in June 1984. Since that time efforts toward source optimization have been ongoing, as well as continuation of the above mentioned cross section measurements.

II. Source Design

The salient features of the ion source are shown in Fig. 1, and summarized in Table I. The source consists of two stages, and is quite similar in size to MINIMAFIOS.[2] The first stage, which supplies plasma to the second stage to facilitate startup, is operated in overdense mode.[3] A helical slow-wave launcher[4] is used to inject 2.45 GHz microwaves into the first stage which is located in an axial magnetic field of 5-7 kG. Plasma density is controlled by the microwave power level and gas pressure, which varies in the 10^{-3} - 10^{-4} torr range. Since microwave absorption in the first stage is non-resonant, the magnetic field can be tuned to optimize second stage performance. The second stage is separated from the first stage by two stages of differential pumping, which is sufficient to maintain low 10^{-6} torr pressure in the second stage during source operation.

In the second stage, electrons confined in a minimum-B configuration are heated by resonant absorption of 10.6 GHz microwaves that are injected radially immediately following the differential pumping section. The minimum-B structure is produced by a superposition of an axial mirror field and a radial hexapole field. Three conventional water-cooled solenoids are used to establish the axial magnetic field profile[5] shown in Fig. 2. The hexapolar field is produced by a compact assembly[6] of $SmCo_5$ permanent magnets positioned around the cylindrical vacuum wall of the second stage. Figure 3 shows a cross sectional view of the 12-piece hexapole magnet assembly, superimposed upon a calculated magnetic field line plot. Cooling of the permanent magnet assembly is achieved by water circulation through the voids created between the cylindrical vacuum wall and the duodecagon defined by the $SmCo_5$ bars.

As regards the mechanical design, care was taken to ensure ease of assembly and access. The sources divides into three sections, each of which is separately supported by, and can be rolled freely on, precision tracks.

The three solenoidal field coils are supported by a similar track structure, and can be moved freely about to expose otherwise inaccessible source parts during source disassembly, or to change the axial mirror ratio in the second stage while the source is fully assembled.

Ion extraction is accomplished by a three-element extraction electrode, the first two elements of which can be biased independently for ion focussing and prevention of electron backstreaming. Position of the anode, extraction electrode, as well as extraction gap can be varied by the use of shims. An electrostatic unipotential lens (operated in accel mode[7]) images the extracted beam onto the entrance slit of a stigmatic 90° magnetic charge analyzer having a 40 cm radius of curvature. The entrance slit assembly is located about 100 cm downstream of the source anode; object and image distances for the 90° magnet are 80 cm. Retractable Faraday cups located immediately after the entrance and exit slits are used to measure total extracted beam currents, and charge selected beam intensities, respectively. Both entrance and exit slit assemblies feature independently adjustable horizontal and vertical slit jaws, to which current can be measured. An electrostatic quadrupole lens located downstream of the exit slits can be used to transport the charge selected beam to those experiments requiring maximum beam intensities.

III. Source Performance

a. 2.45 GHz

Prior to delivery of the 10.6 GHz microwave system, the ECR ion source was operated at an interim frequency of 2.45 GHz. In order to maintain roughly the same ratio of hexapole to axial magnetic field strength at the lower frequency, only 6 of the 12 $SmCo_5$ bars were used, reducing the strength of the hexapole by a factor of two. An additional 25% decrease in hexapole strength was obtained by shimming out the bars to their maximum radius determined by adequate clearance to the solenoidal field windings.

Operation of the source at the lower frequency was far from optimum, due mainly to poor coupling between the second stage plasma and the 2.45 GHz microwaves. Due to their longer wavelength, only a few modes propagated in the second stage cavity; microwave absorption seemed to occur preferentially on the microwave injection side of the second stage which is furthest removed from the extraction region. Even in this mode, the high-charge-state capability of the new source significantly exceeded that of the ORNL PIG ion source. Figure 4 shows a typical charge stage distribution for Ar source gas obtained at this frequency. For light ion production, beams up to fully stripped ^{13}C (10^{-14} el. A) and up to H-like O (10^{-12} el. A) were produced at the lower frequency.

b. 10.6 GHz

Significant improvement in source performance was obtained, as expected, after installation of the 10.6 GHz microwave system, both in terms of total extracted beam intensity and mean charge state of the extracted beams. Microwave absorption increased dramatically, as evidenced by very low reflected power (typically less than 10%) during source operation. Optimum charge state distributions were obtained for a second stage mirror ratio of about 1.6, significantly below the 2.1 mirror ratio attainable at maximum second stage field coil separation. Figure 5 shows a measured charge state distribution obtained for Ar with the source operating at its design frequency of 10.6 GHz. As has been noted by other workers,[8,9] an admixture of O_2 was found to significantly increase the Ar high-charge-state output of the source. Production of light ion beams has yet to be optimized. To date beams of a few electrical microamperes intensity have been obtained of singly charged to He-like ^{13}C and ^{18}O, with intensities dropping to about 30 nA and 3 nA for fully stripped ^{13}C and ^{18}O, respectively.

c. First Stage

In order to isolate the performance of the first stage, measurements of extracted beam intensity were made with the second stage turned off (i.e., with no 10.6 GHz power). In the case of Ar source gas, the overdense first stage plasma produced charge analyzed beams of Ar^{+1} up to 10 microamperes in intensity at 10 kV source potential, with Ar^{+2} and Ar^{+3} down a factor of 4 and 100 in intensity, respectively. Beam currents were stable to within a few percent, and depended mainly on microwave power level and gas pressure, while being relatively insensitive to changes in magnetic field.

Characterizing two-stage operation is less clear-cut. While presence of first stage plasma always seemed to facilitate startup of the second stage, and initially seemed to enhance high charge state production, its effect on total source performance after second stage plasma stabilization appeared to be strongly tuning dependent and non-reproducible. A range of effects due to the first stage were observed, from over a factor of ten improvement to high-charge-state production at one extreme, to significant degradation of high-charge-state performance on the other.

IV. Energy Spread Measurements

In part to try to identify the reason for the erratic effects of the first stage on total source performance, energy spread measurements were carried out on extracted, charge analyzed beams produced under three different source operating conditions: (1) first stage operation alone, (2) second stage operation alone, and (3) two stage operation. The energy spread measurements were made at source voltages of 250, 500, 750, and 1000 V, for Ar ions of charge states +1, +2, +7, and +8. The measurements were performed by scanning a beam of given charge state across the exit slit of the 90° analyzer operated at high resolving power (1 mm entrance and exit slits), and determining the FWHM of the resulting beam profile. Scans using 2×2, 4×4, 6×6, and 8×8 mm entrance and exit slits verified that the beam profile widths were dominated by energy spread of the beam. The results at the four source voltages were extremely consistent, and can be summarized as follows. (1) For first-stage-only operation, energy spreads for Ar^{+1} and Ar^{+2} were measured to be typically (30-40)×q eV, and only slightly dependent on microwave power level or magnetic field. (2) For second-stage-only operation, the measured energy spreads were significantly lower, (6-8)×q eV, again virtually independent of microwave power level. (3) In the case of two-stage operation, the energy spreads roughly double to (14-18)×q eV. It should be noted that, in contrast to the erratic effect noted above of first stage operation on total source performance, the doubling of the energy spread during two-stage operation was observed consistently and reproducibly.

The fact that during two-stage operation the energy spread of Ar^{+1} and Ar^{+2} is about half that observed for first-stage-only operation suggests that ions originating in the first stage play only a minor role in "fueling" the second stage plasma. The observation of the doubling of the energy spread across the whole charge state spectrum during two stage operation compared to second stage only operation nevertheless indicates a definite coupling between stages, possibly through the electrons which are, of course, also injected into the second stage, and which may significantly modify the second stage electron density, as well as other plasma parameters.

V. Cross Section Measurements

Concurrent with source optimization, measurements of total electron capture cross sections for fully stripped light ions incident on atomic hydrogen are in progress. While straightforward experimentally, these measurements are of significant current interest both from a basic and applied scientific perspective, and also provide a convenient mechanism for exploring the capabilities of the new source.

The experiment employs the ORNL atomic hydrogen gas target,[10] a directly heated tungsten tube in which molecular hydrogen is thermally dissociated. A collimation section preceding the target limits the incident beam to a divergence of ±1.7 mr, and 1 mm cross section inside the target. Immediately downstream of the collision target, charge analysis occurs in an electrostatic parallel plate analyzer. A single CEM operated in pulse counting mode is employed for particle detection. The electron capture signal and primary beams are measured alternately for a preselected number of cycles under computer control to determine the total electron capture cross section.

Figures 6 and 7 show results obtained for fully stripped ^{13}C incident on atomic and molecular hydrogen in the energy range 0.23 - 8.3 keV/amu. The error bars shown reflect random uncertainty of the measurement at two standard deviations. Systematic uncertainties are estimated to be ±9% for both the H and H_2 cross sections.[10] Agreement between the present measurements and atomic orbital[11] and molecular orbital[12] calculations is excellent at energies above 2.7 keV/amu. At lower energies, the present results fall as much as 40% below theory. The present results join smoothly with the lower energy measurements of Phaneuf et al.[13]

Total capture cross section measurements are presently under way for $^{18}O^{+8}$ incident on H and H_2, and are planned for $^{15}N^{+7}$, F^{+9}, and Ne^{+10}, in order to systematically study the collisional properties of these true three-body systems as a function of nuclear charge.

Acknowledgments

The author is grateful to D. H. Crandall for initiating the ECR source project, and to R. A. Phaneuf, Y. Jongen, and C. M. Lyneis for helpful discussions and suggestions. It is a pleasure to acknowledge invaluable input by J. W. Johnson to the mechanical source design, and the able technical assistance of J. W. Hale during source assembly and installation. The author is indebted to C. M. Lyneis for providing design details of the LBL ECR source analyzing magnet, and acknowledges the work of A. M. Howald in automating the data acquisition for the cross section measurements.

Table 1. ORNL ECR source parameters.

Microwaves	
First stage 2.45 GHz (300 W max)	50 - 200 W
Second stage 10.6 GHz (2.2 kW max)	20 - 800 W
Magnetic Fields	
Mirror ratio	1.6
Hexapole field at vacuum wall	4.0 kG
Field in extraction plane	4.5 kG
Field in first stage	5 - 7 kG
Total solenoid power	60 kW
Vacuum (operating condition)	
First stage	10^{-3} - 10^{-4} T
Second stage (1×10^{-7} torr base)	1 - 6×10^{-6} T
Extraction	1×10^{-7} T
Beamline (2×10^{-9} torr base)	2×10^{-8} T
Dimensions	
Solenoids ID	18 cm
Solenoids OD	40 cm
Hexapole ID	9.5 cm
Hexapole length	33 cm
Vacuum wall ID second stage	8.6 cm
Anode aperture	0.5 cm
Extraction aperture	0.8 cm
Extraction gap	2.6 cm

References

1. J. Arianer and R. Geller, Ann. Rev. Nucl. Part. Sci. 31, 19 (1981).
2. R. Geller, B. Jacquot, and C. Jacquot, Proceedings of the 7th Symposium (1983 International) on Ion Sources and Ion Assisted Technology - ISIAT 1983, p. 187, Kyoto, Japan.
3. G. Lisitano, M. Fontanesi, and E. Sindoni, Appl. Phys. Lett. 16, 122 (1970).
4. D. P. Grubb and T. Lovell, Rev. Sci. Inst. 49, 77 (1978).
5. The field profile shown in Fig. 2, showing a second stage mirror ratio of 2.1, is obtained at maximum second stage coil separation, and thus does not accurately represent the optimized profile found for 10.6 GHz operation with 1.6 mirror ratio.
6. K. Halbach, Nucl. Inst. Meth. 169, 1 (1980).
7. Operation in decel mode is not possible in the present application due to the favorable conditions for Penning discharge produced by the combination of ion source magnetic fringe field and lens electrostatic field.
8. H.-G. Mathews, H. Beuscher, R. Fiedler, and W. Krauss-Vogt, IKP - Annual Report 1983, KFA Juelich.
9. D. J. Clark, Y. Jongen, and C. M. Lyneis, Proceedings of 10th Int. Conf. on Cyclotrons, East Lansing, Mich.; to appear in IEEE Trans. on Nucl. Sci., August 1984.
10. R. A. Phaneuf, F. W. Meyer, and R. H. McKnight, Phys. Rev. A17, 534 (1978).
11. W. Fritsch and C. D. Lin, Phys. Rev. A29, 3039 (1984).
12. T. A. Green, E. J. Shipsey, and J. C. Browne, Phys. Rev. A25, 1364 (1982).
13. R. A. Phaneuf, I. Alvarez, F. W. Meyer, and D. H. Crandall, Phys. Rev. A26, 1892 (1982).

Figure Captions

Fig. 1. The ORNL ECR multicharged ion source.

Fig. 2. Magnetic field on-axis versus axial positions; locations of solenoidal field coils and ECR region are indicated.

Fig. 3. Calculated radial cross section of hexapole magnetic field lines showing positions and magnetic orientation of $SmCo_5$ bars.

Fig. 4. Ar charge state distribution - 2.45 GHz source operation.

Fig. 5. Ar charge state distribution - 10.6 GHz source operation.

Fig. 6. Present results of total electron capture cross section measurements for $^{13}C^{+6}$ incident on atomic hydrogen as a function of energy.

Fig. 7. Present results of total electron capture cross section measurements for $^{13}C^{+6}$ incident on molecular hydrogen as a function of energy.

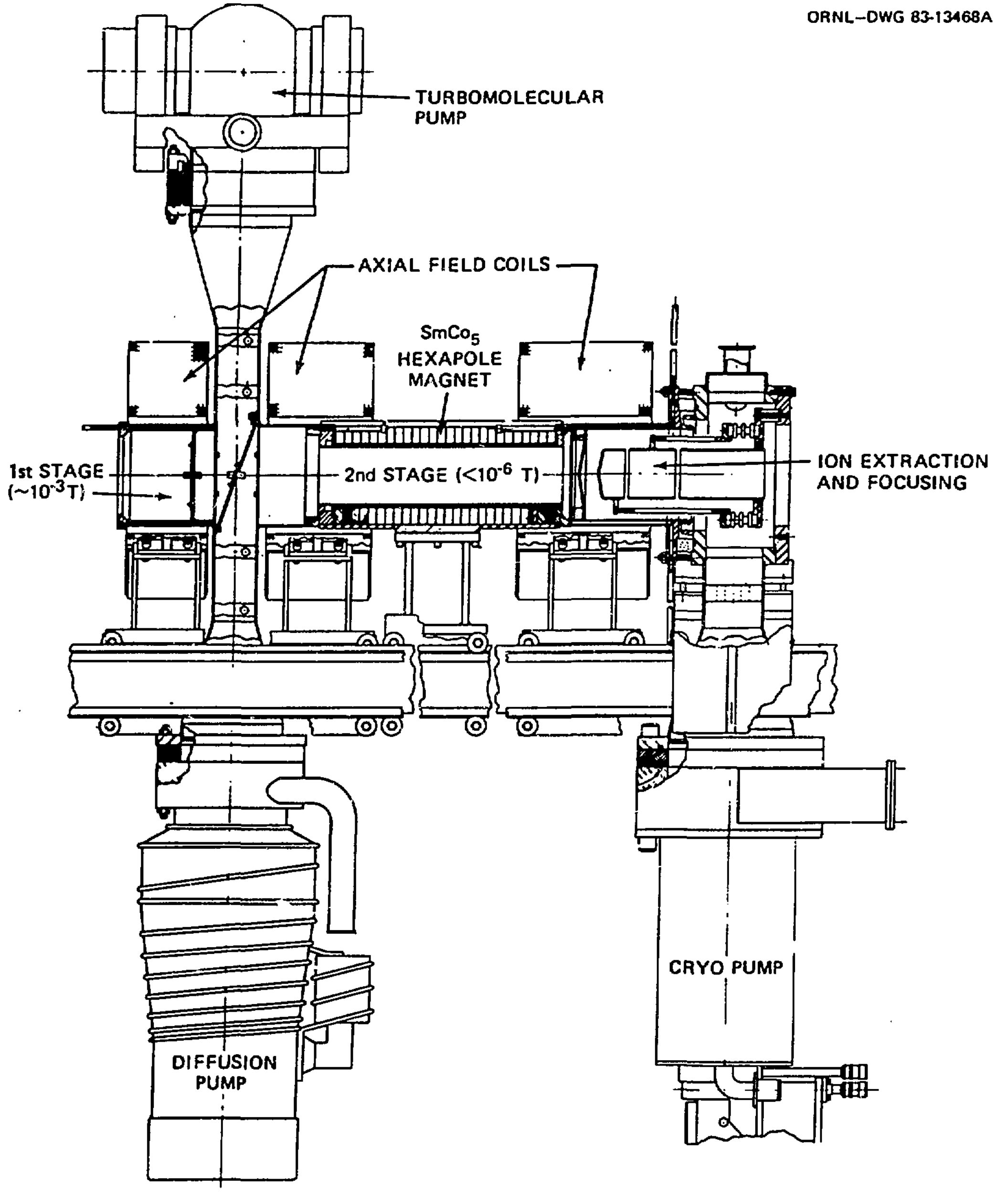
ORNL–DWG 83-13468A
TURBOMOLECULAR PUMP
AXIAL FIELD COILS
$SmCo_5$ HEXAPOLE MAGNET
1st STAGE (~10^{-3}T)
2nd STAGE (<10^{-6} T)
ION EXTRACTION AND FOCUSING
DIFFUSION PUMP
CRYO PUMP

Fig. 1

ORNL–DWG 83-17376

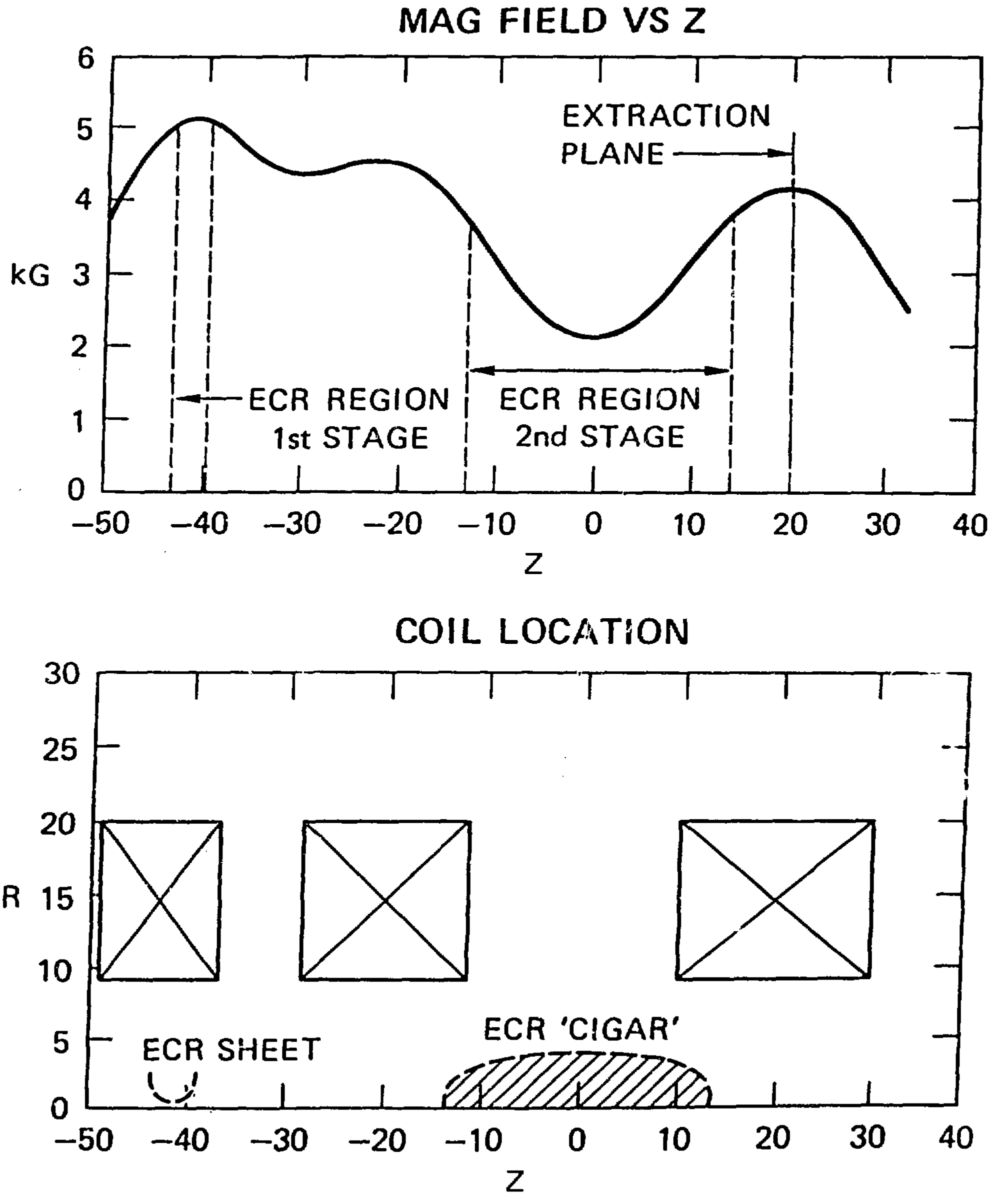

Fig. 2

ORNL–DWG 83-17665

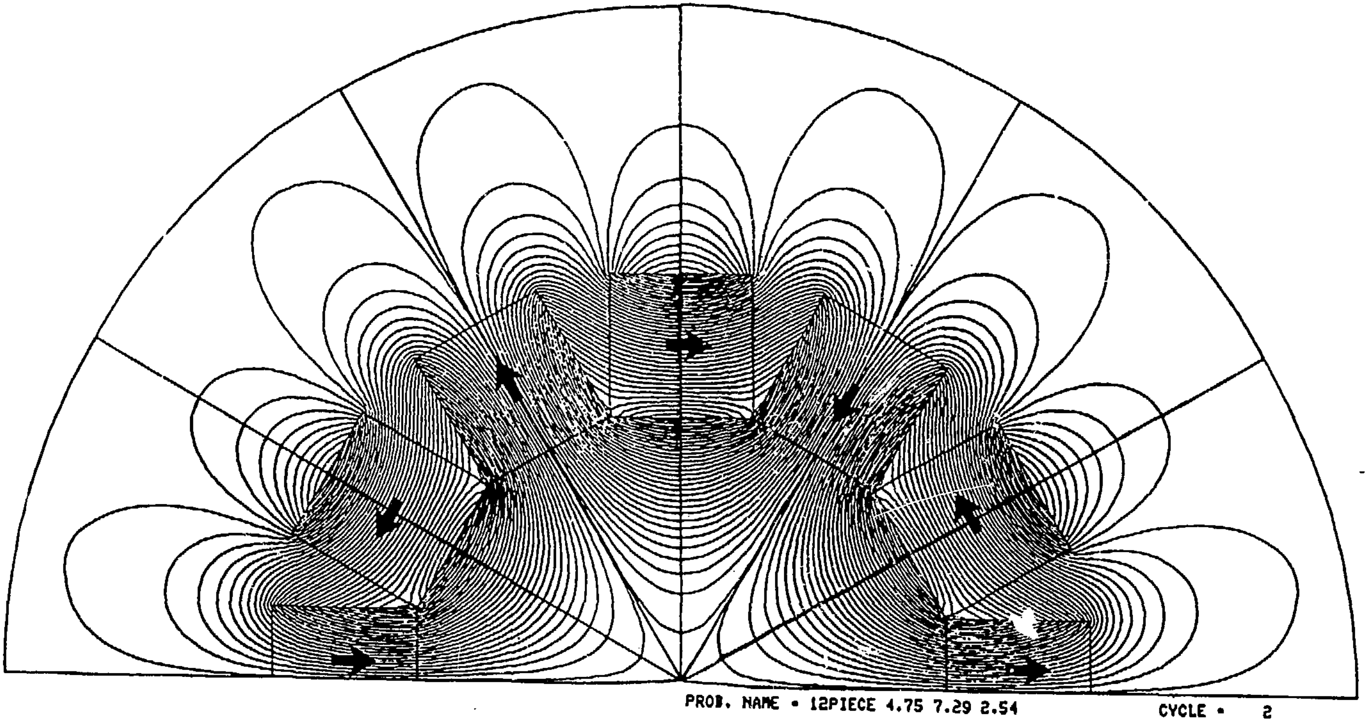

Fig. 3

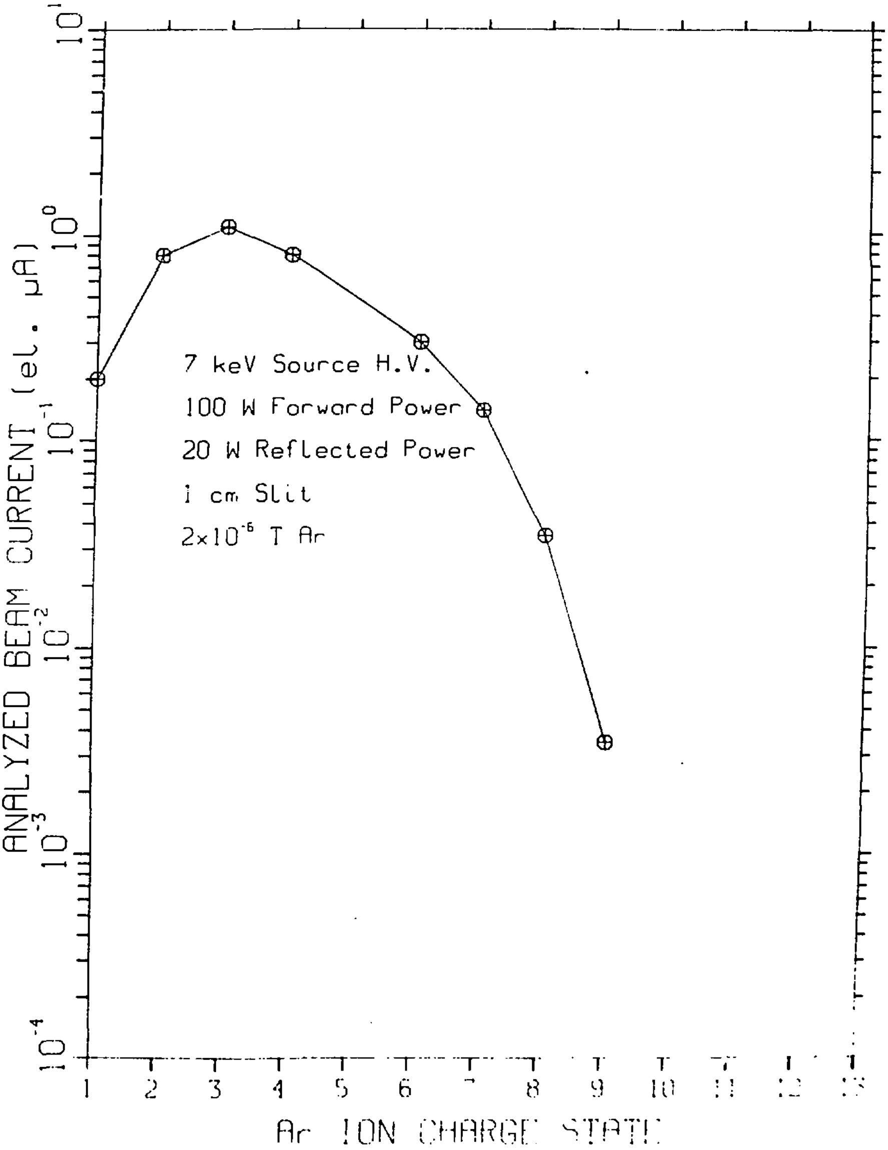
ANALYZED BEAM CURRENT (el. μA)
Ar ION CHARGE STATE
10^{1}
10^{0}
10^{-1}
10^{-2}
10^{-3}
10^{-4}
1
2
3
4
5
6
7
8
9
10
11
12
13
7 keV Source H.V.
100 W Forward Power
20 W Reflected Power
1 cm Slit
2×10^{-6} T Ar

Fig. 4.

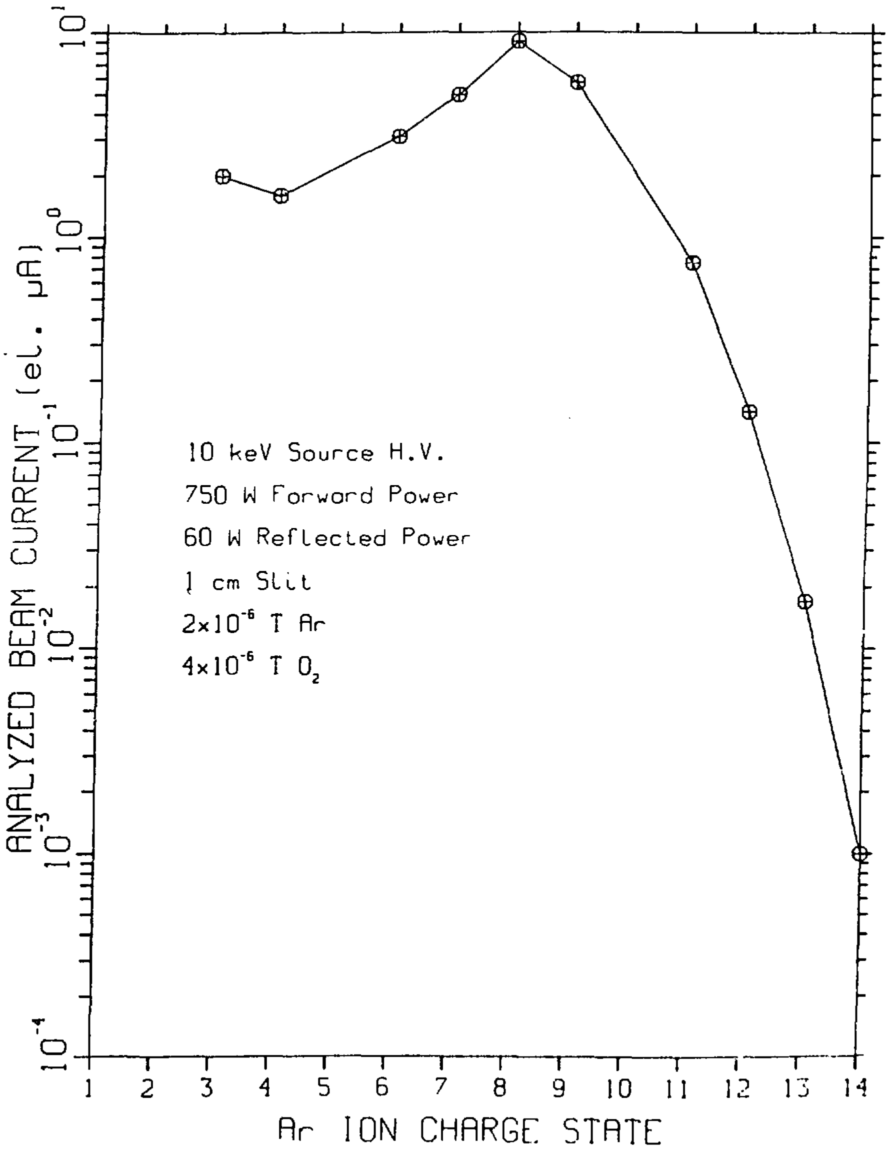

10^1
10^0
10^{-1}
10^{-2}
10^{-3}
10^{-4}
ANALYZED BEAM CURRENT (el. μA)
10 keV Source H.V.
750 W Forword Power
60 W Reflected Power
1 cm Slit
2×10^{-6} T Ar
4×10^{-6} T O_2
1
2
3
4
5
6
7
8
9
10
11
12
13
14
Ar ION CHARGE STATE

Fig. 5

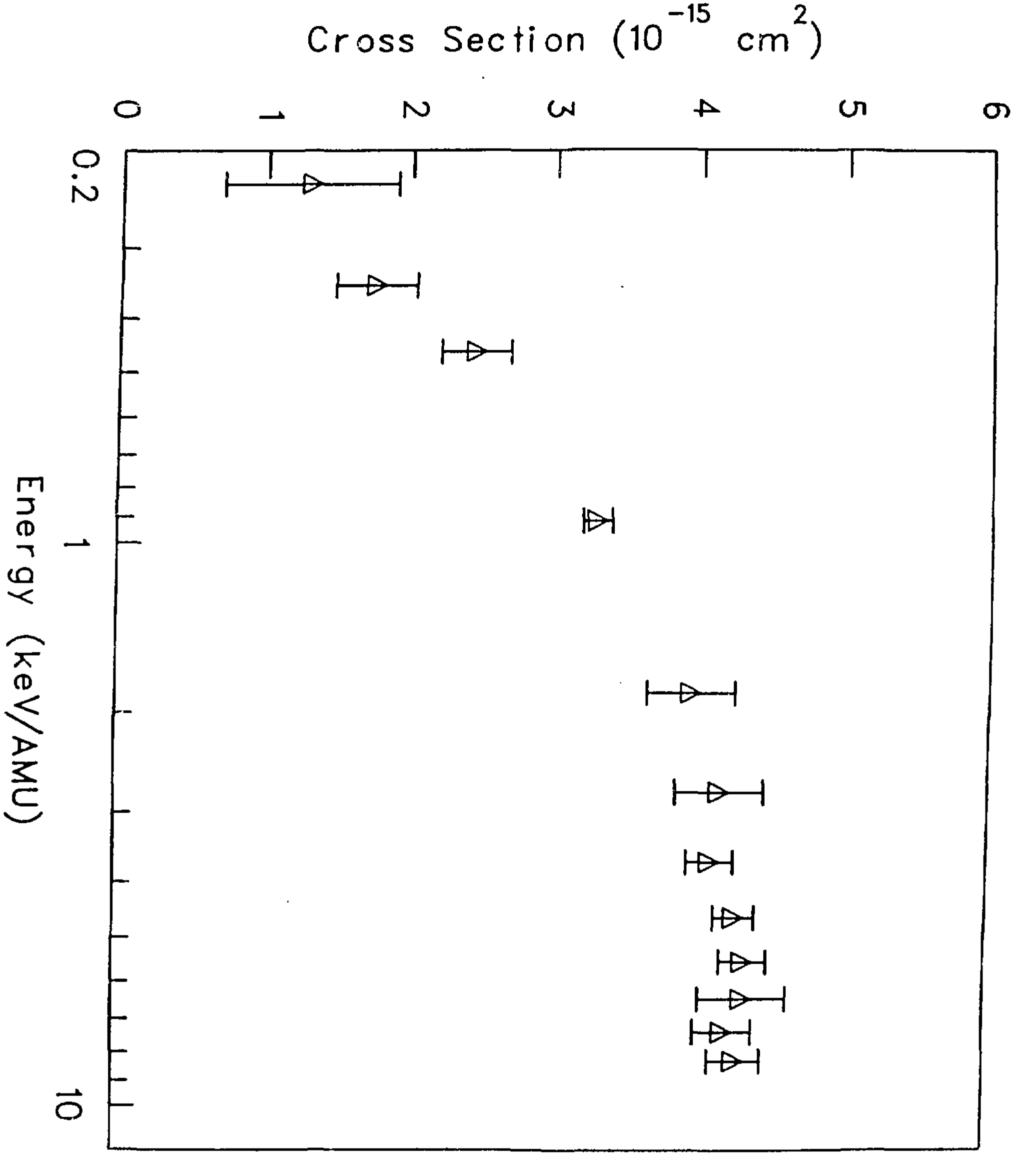

Fig. 6

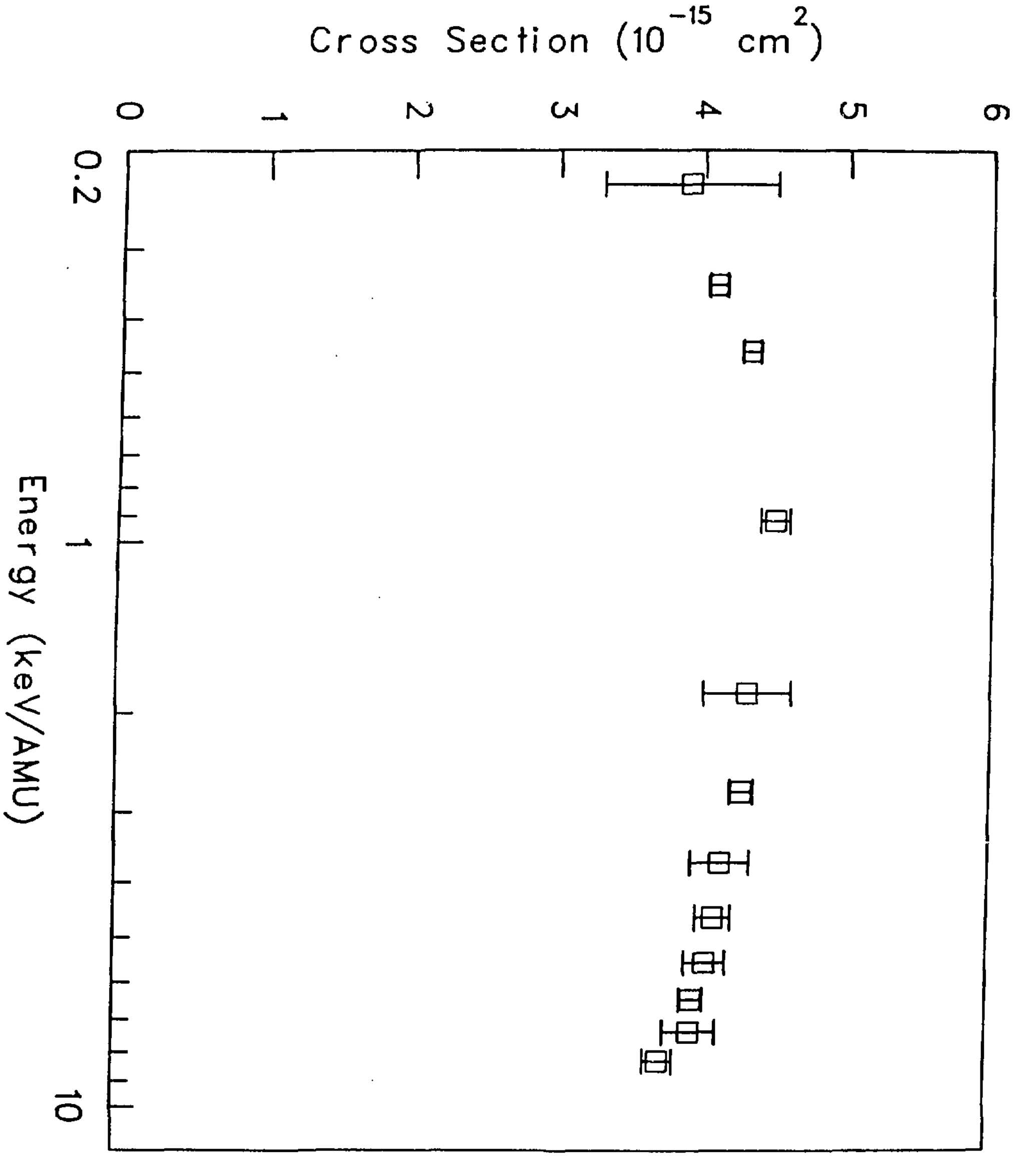

Fig. 7